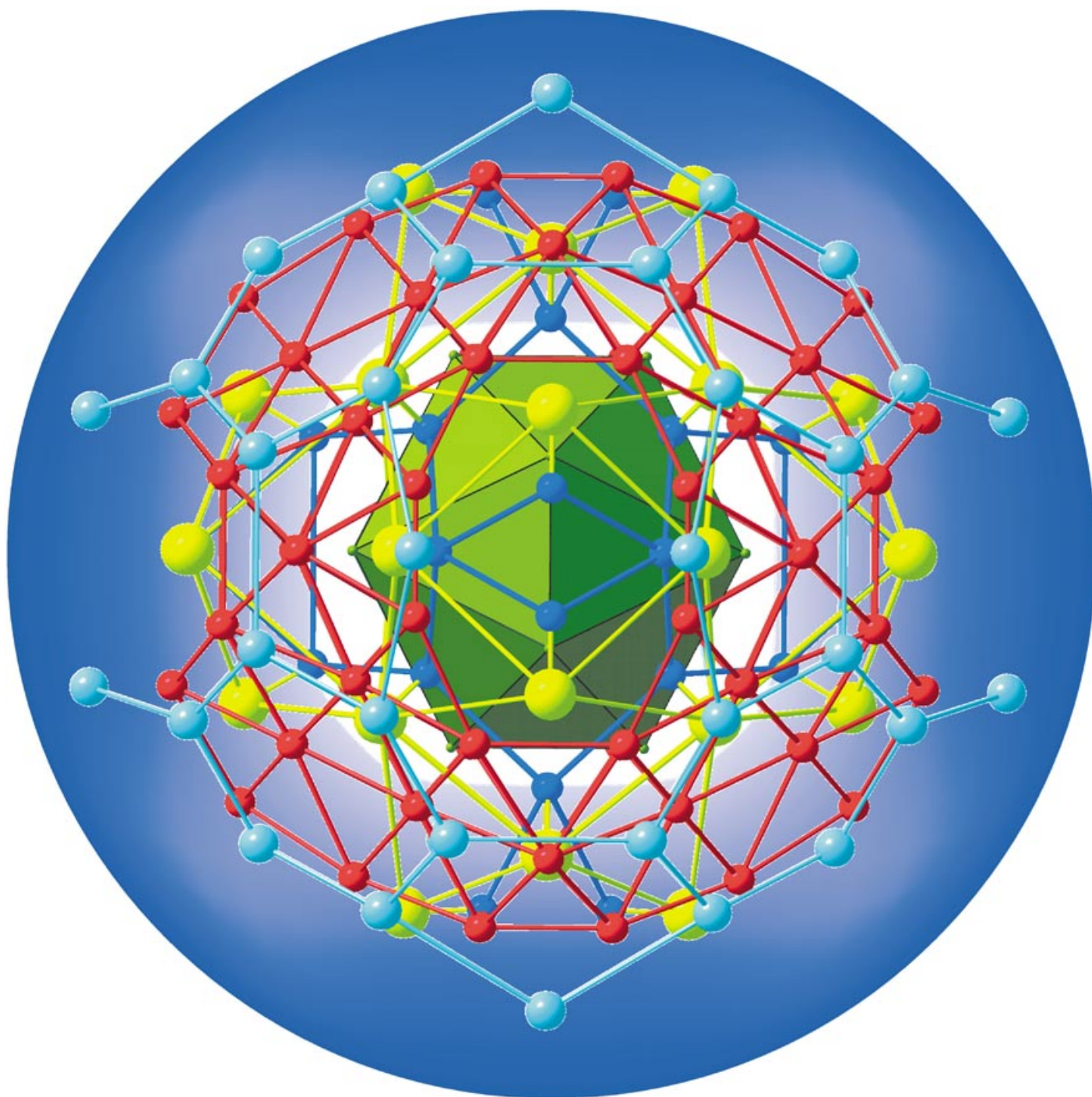


# Zuschriften



Dem unendlichen kationischen Te-Ni-Oxohalogenid-Netz, das M. Johansson et al. in ihrer Zuschrift auf den folgenden Seiten beschreiben, liegt eine Folge gleichatomiger, kovalent verbundener „Zwiebelschalen“ zugrunde. Die äußeren Ni-Atome (hellblau) bilden Buckminsterfulleren-artige Cluster, die in einer kubisch innenzentrierten Packung mit acht Nachbarn verknüpft sind.

## Host–Guest Compounds in the Family of Tellurium–Nickel Oxohalogenides\*\*

Mats Johansson,\* Sven Lidin, Karl W. Törnroos, Hans-Beat Bürgi, and Patrice Millet

Some elements with stereochemically active lone pairs show a strong propensity in their oxohalogenides to agglomerate with halogenide ions, thus forming clusters, rods or lamellar assemblies, to bond covalently to an oxidic matrix, and to spatially separate one from the other.<sup>[1]</sup> This behavior mimics that of water–amphiphile–oil systems not only structurally, but also in the sense that the oxohalogenides may be manipulated similarly by using chalcophile or halophile metals to swell the oxide or halide volume. We have recently described the planar layer structures of  $[\text{Ni}_5(\text{TeO}_3)_4]\text{Cl}_2$  and  $[\text{Ni}_5(\text{TeO}_3)_4]\text{Br}_2$ , the first oxohalogenide phases that contain  $\text{Te}^{\text{IV}}$  ions in combination with  $\text{Ni}^{\text{II}}$  ions.<sup>[2]</sup> To our knowledge only three other oxide phases that contain  $\text{Te}^{\text{IV}}$  ions in combination with  $\text{Ni}^{\text{II}}$  ions have been described before, namely  $\text{NiTe}_2\text{O}_5$ ,  $\text{Ni}_2\text{Te}_3\text{O}_8$ , and  $\text{Ni}_3(\text{OH})_2(\text{TeO}_3)_2$ .<sup>[3–5]</sup>

Herein we present the synthesis of three products within this new family of compounds with the idealized composition  $[\text{Te}_{32}\text{Ni}_{30}\text{X}_3\text{O}_{90}]^{5+}[\text{Ni}_4\text{X}_{13}]^{5-}$ . The anionic part of the products discloses further dimensions of complexity and necessitates a division of the three structures into two types. The first type is represented by  $[\text{Te}_{32}\text{Ni}_{30}\text{Br}_{2.64}\text{O}_{90}][\text{Ni}_{3.39}\text{Br}_{12.14}]$  (**1a**) and  $[\text{Te}_{32}\text{Ni}_{30}\text{Cl}_{2.69}\text{O}_{90}][\text{Ni}_{3.10}\text{Cl}_{11.52}]$  (**1b**); the second type is represented by  $[\text{Te}_{32}\text{Ni}_{30}\text{Cl}_{2.67}\text{O}_{90}][\text{Ni}_{4.48}\text{Cl}_{15.78}]$  (**2**). These new phases form only at relatively high temperatures, above

800 K. All attempts to produce the compounds as single phases have been unsuccessful, and the reaction product is always a mixture of the title compounds and a matrix of  $[\text{Ni}_5(\text{TeO}_3)_4]\text{X}_2$ .<sup>[2]</sup> Therefore all crystals subject to analyses were selected manually on the basis of color and morphology. All three compounds crystallize in the cubic system, space group  $Im\bar{3}$  (no. 204). Results of stoichiometric analyses by energy-dispersive spectrometry (EDS) and X-ray diffraction (XRD) are compared in Table 1.

Table 1: Elemental analysis for **1a**, **1b**, and **2**.<sup>[a]</sup>

Compound	<b>1a (X = Br)</b>		<b>1b (X = Cl)</b>		<b>2 (X = Cl)</b>	
	EDS	XRD	EDS	XRD	EDS	XRD
Te	40.6 ± 0.6	39.9	39.6 ± 0.7	40.4	39.0 ± 1.4	37.7
Ni	41.0 ± 0.7	41.7	41.1 ± 0.9	41.7	40.4 ± 1.7	40.6
X	18.4 ± 0.7	18.4	19.3 ± 0.7	17.9	20.5 ± 1.9	21.7

[a] Results of EDS analyses are averages of determinations on ten different crystals. XRD results were obtained from refined compositions (in %, O atoms not included).

Both types of compounds contain covalently bonded, cationic entities of approximate composition  $[\text{Te}_{32}\text{Ni}_{30}\text{X}_3\text{O}_{90}]^{5+}$  (X = Br, Cl), which form an infinite porous network enclosing large cavities that contain guests of anionic clusters. The cationic network is effectively identical for all three compounds, whereas the anionic guest clusters differ from compound to compound.

The cationic clusters may be considered as being built from a sequence of homoatomic, concentric onion skins. The outermost shell is a Buckminster Fullerene-like polyhedron of 60 Ni atoms. It shares hexagons along the [111] direction and edges along the [100] direction with neighboring  $\text{Ni}_{60}$  units. The simultaneous contacts along [111] and [100] reduce the symmetry of the Fullerene-like shells from icosahedral to cubic. The Ni atoms may be considered as sitting on a P-type minimal surface that defines the interface between individual spheres of a bcc packing (Figure 1). The Ni atoms surrounded

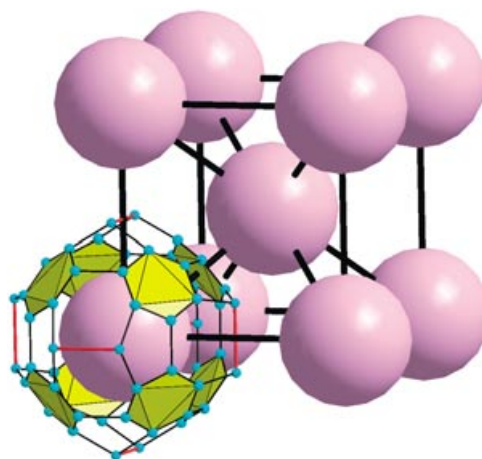


Figure 1. One Buckminster Fullerene-like  $\text{Ni}_{60}$ -cluster with violet skins indicating the subsequent inner shells of atoms (O and Te) and the innermost central anionic cluster. The bcc packing of the spherical shells is indicated by black lines.<sup>[6]</sup>

[\*] Dr. M. Johansson, Prof. Dr. S. Lidin  
Department of Inorganic chemistry, Stockholm University  
S-106 91 Stockholm (Sweden)  
Fax: (+46) 8-152187  
E-mail: matsj@inorg.su.se

Prof. K. W. Törnroos  
Department of Chemistry, University of Bergen  
Allégt. 41, 5007 Bergen (Norway)

Prof. Dr. H.-B. Bürgi  
Laboratorium für Kristallographie, Universität Bern  
Freiestr. 3, 3012 Bern (Switzerland)

Dr. P. Millet  
Centre d'Elaboration de Matériaux et d'Etudes Structurales  
(CEMES/CNRS)  
29 rue Jeanne Marvig, BP 4347, Toulouse Cedex 4 (France)

[\*\*] We thank Mr. Marian Mikus at Sandvik Coromant AB for the microsond analyses and Dr. Javier Garcia-Garcia at Stockholm University for the TEM study. This work has been carried out in part through financial support from the Swedish Research Council and the European Union (HPHN-CT-2002-00193).



by the coordinating O atoms are given in polyhedral representation in Figure 2. Each  $\{\text{NiO}_6\}$  octahedron share edges with two other  $\{\text{NiO}_6\}$  octahedra, six of which form a ring of composition  $\{\text{Ni}_6\text{O}_{24}\}$ . The  $\{\text{Ni}_6\text{O}_{24}\}$  units also share corners

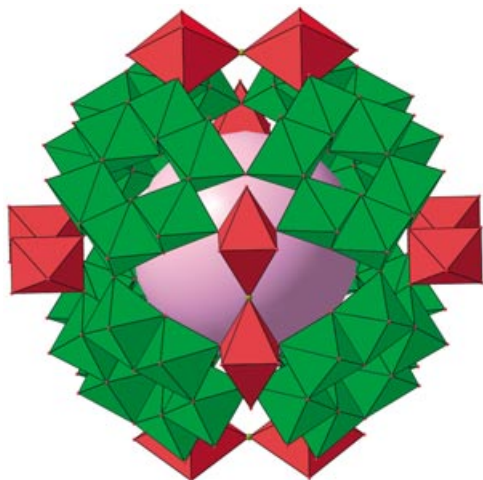


**Figure 2.** The Ni shell together with the inner and outer O shells in a polyhedral representation. The ringlike  $\{\text{Ni}_6\text{O}_{24}\}$  units built up from  $\{\text{NiO}_6\}$  octahedra (green) share corners with the dimeric units  $\{\text{O}_5\text{Ni-X-NiO}_5\}$ ; the two octahedra (red) of the dimer share a halogen atom (brown). Together the green and red polyhedra enclose the subsequent Te shell and the central anionic cluster, both indicated as a violet sphere.

with the  $\{\text{NiO}_5\text{X}\}$  octahedra, which themselves are connected into dimers through a shared halide ion X. The distance between these two Ni atoms is much longer than between the other Ni atoms. This spherical arrangement of sixty coordinated Ni ions surrounds a shell of O atoms, which in turn envelopes the shell that contains Te atoms and the cavities hosting the anionic guest clusters.

The O atoms that line the inside of the Ni shell form an intriguing arrangement in itself, being close-packed on a curved surface (Figure 3). It may thus be considered as a 3D curved variant of the planar layer structures that figure so prominently among halide compounds with available lone pairs.<sup>[7]</sup>

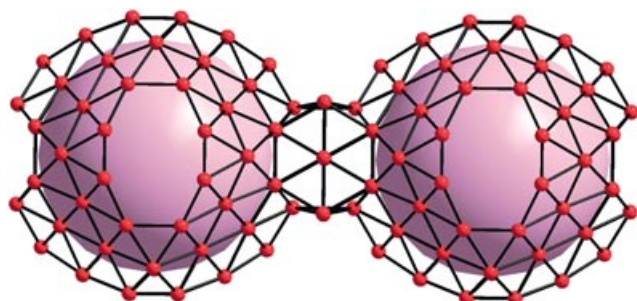


**Figure 3.** A close-packed layer of oxygen atoms envelopes both sides of the Ni substructure (See Figure 2). The innermost layer of O atoms is shown. The violet skins indicate the next shell of atoms, Te, and the anionic cavity inside of this O layer.

Thirty two Te atoms form the third shell of the structure and constitute the boundary of the cavity for the anionic guests. The Te atoms come in three groups with different center-to-vertex distances (Figure 4). The first group, which is

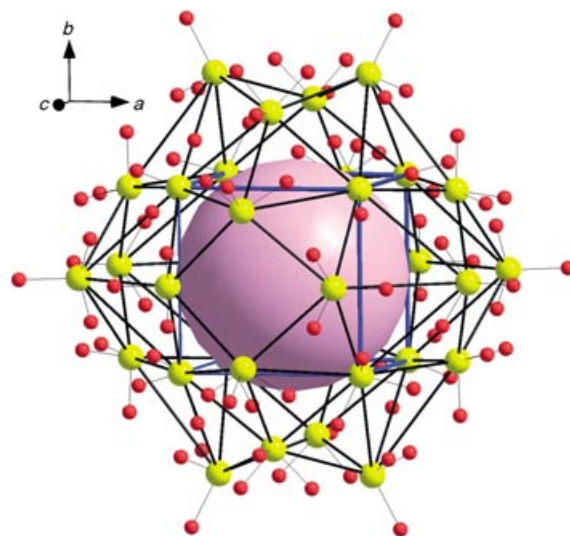


**Figure 4.** The Te shell (yellow) found inside the innermost layer of O atoms (red). The 24 Te atoms furthest away from the center of the onion form a distorted truncated octahedron, outlined with thick black lines. The eight innermost Te atoms form a cube emphasized by blue edges. The central cavity containing an anionic cluster is marked with a violet sphere.

closest to the center of the cavity with a center-to-vertices distance of 5.5 Å, forms a cube. The second shell at 6.5 Å forms a distorted icosahedron. These two groups of Te atoms have their lone pairs pointing towards the center of the cavity. The third group at 7.4 Å forms another icosahedron, but the lone pairs are clearly pointing away from the center (Figure 5a) and towards the bridging halogen atoms ( $\{\text{NiO}_5\text{X-NiO}_5\}$ ; Figure 2 and Figure 4). The two groups with the longer distances may also be viewed as constituting the corners of a deformed truncated octahedron.

The description above is, however, somewhat simplified. In fact, the population of the halogen X in the  $\{\text{O}_5\text{NiXNiO}_5\}$  dimer is diminished so that the actual population of X is smaller than unity, 0.88 and 0.90 in **1a** and **1b**, respectively. Concurrently, the group of most-distant Te atoms from the center (Te3) are disordered over two positions of which the one with the larger population is shown in Figure 4. The minor Te site with a population between 0.10 and 0.12 is displaced towards the center of the cavity by 0.35 to 0.5 Å, depending on the compound. Disorder in the cationic cluster is thus modest.

The situation inside the cavities is both more complex and more variable than that in the host network. In compound **1a**, 12 Br atoms form an almost perfect icosahedron with crystallographic  $m\bar{3}$  ( $T_h$ ) symmetry and surround a central Br ion reminiscent of the  $\{\text{Hg}_5\text{Cl}_{13}\}$  arrangement in  $\text{Hg}_{11}\text{Ca}_2\text{Cl}_{26}(\text{H}_2\text{O})_{16}$ .<sup>[8]</sup> The 20 triangular faces of the Br icosahedron are capped by the 8 lone pairs of the Te atoms forming a cube and 12 lone pairs of the closer of the two Te

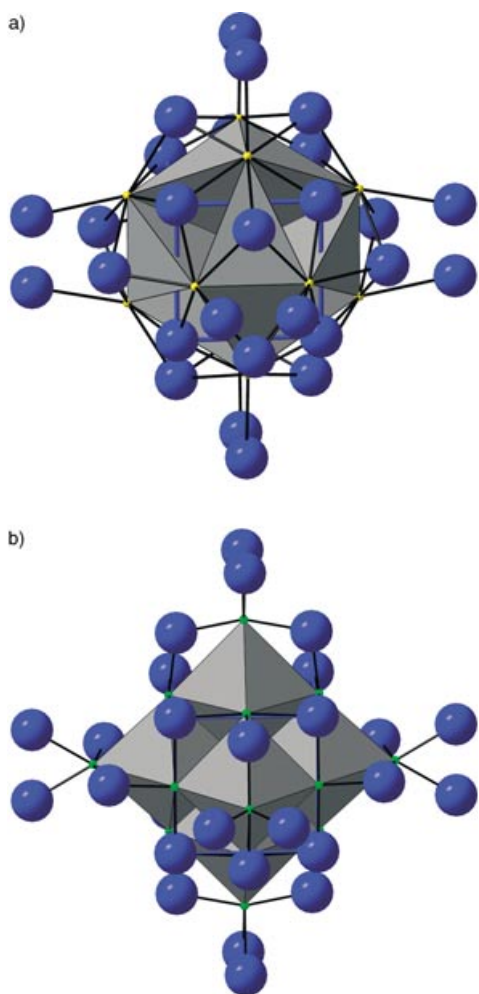


**Figure 5.** a) The icosahedral  $\{X_{13}\}$  cluster found in **1a** and **1b**, surrounded by Te lone pairs (blue). The twelve closed tetrahedra (gray) host the Ni atoms, but only three or four tetrahedra are occupied in any given cavity. Note that the eight lone pairs forming an inner cube cap the faces of empty tetrahedra, while the lone pairs capping the filled tetrahedra are further away. X atoms (Br or Cl) in light brown. b) The  $\{Cl_{19}\}$  cluster found in **2** surrounded by Te lone pairs (blue). The six closed octahedra (gray) host one Ni atom each. Note the eight lone pairs that form a cube cap the empty tetrahedra between the  $\{NiCl_6\}$  octahedra. Twelve lone pairs sit over the edges of the octahedra and another 12 are further away. Cl atoms are in green.

icosahedra. The second set of Br triangles together with the central Br constitute 12 tetrahedral cavities that host Ni atoms (Figure 5a). The refined composition of the cavity is  $[Ni_{3.39}Br_{12.14}]^{5.36-}$ , thus implying that only three or four Ni atoms reside in any given cavity and that there is a slight deficit of Br ions (12.1 versus 13). It is, however, not possible to determine the exact local arrangements of atoms in this cluster from the X-ray diffraction data.

For the relatively large Br ion in **1a**, only the icosahedral guest cluster described above has been observed. For the smaller  $Cl^-$  ion, other configurations are allowed. Specifically in compound **2**, if the rock-salt structure is assumed, approximately half of the icosahedra clusters are replaced by a  $\{Ni_6Cl_{19}\}$  fragment. A central  $Cl^-$  ion is surrounded by a

$Ni_6$  octahedron, each of which is itself octahedrally coordinated by  $Cl^-$  ions (Figure 5b). An analogous  $[V_6O_{19}]$  cluster has recently been observed in an alkoxo-oxovanadium compound.<sup>[9]</sup> The remaining half of the cavities is filled with a  $[Ni_3Cl_{12.78}]$  cluster that is similar to the  $[Ni_{3.39}Br_{12.14}]$  cluster described above for **1a**. The sum of the negative charges of these two clusters in **2** exceeds the positive charge of the surrounding cationic framework.

The anionic cluster in the chloride compound **1b**, synthesized from a flux containing KCl in addition to  $NiCl_2$ , has the composition  $[Ni_{3.10}Cl_{11.52}]^{5.31-}$ . Atomic positions as well as the Ni:Cl ratio are very similar to that in **1a** (0.28 versus 0.27), but the cluster occupies only about 90% of the cavities. Electron-density-difference maps show indications of the rock-salt-like  $[Ni_6Cl_{19}]$  cluster, but its occupancy is too low to be included in a meaningful least-squares refinement of the X-ray data.

These complex disorder patterns raise questions about the exact composition of the compounds reported and the possibility of locally lowered crystal symmetry. Selected-area electron-diffraction studies, however, give no indication of locally lowered symmetry and it may be assumed that symmetry breaking in one cavity has negligible effect on neighboring cavities.

The EDS data in Table 1 agree within experimental uncertainties with the populations obtained by X-ray diffraction. For **1a** and **1b**, these populations were obtained with the constraint that the crystal be electroneutral resulting in final compositions of  $[Te_{32}Ni_{30}Br_{2.64}O_{90}]^{5.36+}[Ni_{3.39}Br_{12.14}]^{5.36-}$  and  $[Te_{32}Ni_{30}Cl_{2.69}O_{90}]^{5.31+}[Ni_{3.10}Cl_{11.52}]^{5.31-}$ , respectively. Refinements without this constraint tend to increase the halogen content by about 0.7, thus implying excess negative charge. Improvement in the confidence factors is minor, typically  $\approx 0.1\%$  in  $\Delta R1$ . The unconstrained charges in the cationic and anionic clusters of **2** clearly match less well, namely,  $[Te_{32}Ni_{30}Cl_{2.67}O_{90}]^{5.33+}$  versus  $[Ni_{4.48}Cl_{15.78}]^{6.82-}$ . However, the imposition of an electroneutrality constraint on the crystallographic refinement of **2** results in an unreasonable increase in confidence factors, from  $R1 = 2.8\%$  to  $4.2\%$ .

The consistent tendency towards excess negative charge in crystallographic refinements of all three compounds could be related to the pronounced disorder in the anionic cluster, which makes it difficult to model the electron density under the constraint of electroneutrality. Overestimation of halogen content coupled with an overestimation of thermal or disorder smearing is but one of the explanations of our observations; underestimation of the Ni population is another. In addition, the difficulty of doing an exact absorption correction in the presence of elements as heavy as Te also adds a degree of uncertainty with respect to the population factors of the lighter elements.

The coordination of the individual atoms in the host structure is standard and depends little on the halogen type. The two crystallographically different Ni sites in the  $[Ni_6O_{24}]$  rings show nearly regular octahedral coordination to the O atoms. The coordination of the octahedra in the  $\{O_5NiXNiO_5\}$  dimer is better described as square-planar with four normal Ni–O distances, 2.021(3)–2.031(4) Å, in a plane and long distances to the halogen (Cl, Br), 2.511(1)–2.567(2),

2.629(2) Å, and O atoms, 2.44(1)–2.582(9) Å, perpendicular to that plane.

The Te atoms all exhibit a classical coordination polyhedron denoted {TeO<sub>3</sub>E} formed by three O atoms and a lone pair E. The TeO<sub>3</sub> distances range from 1.880(5) to 1.916(3) Å and the bond angles from 82.9(2) to 101.4(1)°; individual values for specific Te atoms are similar within the statistical uncertainty among the three compounds. All O atoms of the {TeO<sub>3</sub>E} tetrahedra are shared with the Ni-centered octahedra.

Given the variety of the observed structures and compositions of the central anionic clusters, compounds **1a**, **1b**, and **2** likely constitute the first members of a new family of inorganic supramolecular compounds,<sup>[10]</sup> in which the cavities of the peculiarly shelled covalent network could host various other anionic clusters consisting of, for example, Mo, Mn, Hg, or Cu atoms in combination with halogen atoms.

## Experimental Section

All compounds were synthesized by chemical-transport reactions in sealed evacuated glass tubes. The starting materials were NiO (Avocado Research Chemicals Ltd.), NiCl<sub>2</sub> (Merck, >98% anhydrous), NiBr<sub>2</sub> (Strem Chemicals, 99+%), KCl (Merck, p.a.) and TeO<sub>2</sub> (Strem Chemicals, 99+%).

Compound **1a** was synthesized from a mixture of NiO:NiBr<sub>2</sub>:TeO<sub>2</sub> in a molar ratio of 3:1:3 at 823 K for 65 h producing pale brown small cubic crystals. Compound **1b** was synthesized from a mixture of NiO:NiCl<sub>2</sub>:TeO<sub>2</sub>:KCl in a molar ratio of 2:2:3:2 kept at 873 K for 40 h yielding green cubic crystals. For compound **2**, a mixture of NiO:NiCl<sub>2</sub>:TeO<sub>2</sub> in a molar ratio of 4:1:4 was kept at 873 K for 40 h yielding green cubic crystals. The products were characterized with a scanning electron microscope (SEM, JEOL 820) and with an energy-dispersive spectrometer (EDS, LINK AN10000). The latter confirmed the presence and stoichiometry of Ni, Te, Cl, and Br (Table 1). EDS and microprobe analysis (JEOL JXA8900R) at 10, 15, and 20 kV conclusively proved the absence of Na, Si or K contaminations.

The single crystal X-ray data were collected on a Bruker-AXS SMART 2 K CCD diffractometer equipped with an Oxford Cryostream series 600 crystal cooling system, MoK<sub>α</sub> radiation, λ = 0.71073 Å, graphite monochromator. A full reflection sphere was collected by means of 0.3° ω-scans by using SMART and reduced by using SAINT.<sup>[11,12]</sup> Gaussian face-indexing absorption correction, structure solution, and refinement were made with SHELXTL.<sup>[13]</sup> The lone-pair positions were calculated in geometrically idealized positions 1.25 Å away from the Te atoms.

**1a:** Crystal size: 0.074 × 0.074 × 0.064 mm, *T* = 100 K, cubic *Im* $\bar{3}$ , *a* = 17.5077(9) Å, *V* = 5366.5(5) Å<sup>3</sup>, *Z* = 2, ρ<sub>calc</sub> = 5.45 g cm<sup>-3</sup>, 2θ<sub>max</sub> = 54.22°, 33882 integrated reflections, 1093 unique, *R*<sub>int</sub> = 0.0663, 104 parameters, μ = 20.40 mm<sup>-1</sup>, *R*1 [*I* > 2σ(*I*)] = 0.0213, *wR*2 (all data) = 0.0512, *S* = 1.07, largest difference peaks 1.08/−1.46 e Å<sup>-3</sup>.

**1b:** Crystal size: 0.104 × 0.125 × 0.154 mm, *T* = 123 K, cubic *Im* $\bar{3}$ , *a* = 17.4549(8) Å, *V* = 5318.0(4) Å<sup>3</sup>, *Z* = 2, ρ<sub>calc</sub> = 4.75 g cm<sup>-3</sup>, 2θ<sub>max</sub> = 65.08°, 47467 integrated reflections, 1762 unique, *R*<sub>int</sub> = 0.0355, 104 parameters, μ = 14.11 mm<sup>-1</sup>, *R*1 [*I* > 2σ(*I*)] = 0.0285, *wR*2 (all data) = 0.0573, *S* = 1.307, largest difference peaks 2.20/−1.99 e Å<sup>-3</sup>.

**2:** Crystal size: 0.125 × 0.119 × 0.100 mm, *T* = 153 K, cubic *Im* $\bar{3}$ , *a* = 17.5443(3) Å, *V* = 5400.2(2) Å<sup>3</sup>, *Z* = 2, ρ<sub>calc</sub> = 4.97 g cm<sup>-3</sup>, 2θ<sub>max</sub> = 65.44°, 26545 integrated reflections, 1771 unique, *R*<sub>int</sub> = 0.0358, 109 parameters, μ = 14.75 mm<sup>-1</sup>, *R*1 [*I* > 2σ(*I*)] = 0.0278, *wR*2 (all data) = 0.0498, *S* = 1.21, largest difference peaks 1.25/−1.27 e Å<sup>-3</sup>.

The unit cells and the space group were confirmed from X-ray powder diffraction patterns obtained in a Guinier–Hägg focusing camera with subtraction geometry and CuK<sub>α1</sub> radiation (λ =

1.54060 Å). Finely powdered Si [*a* = 5.43088(4) Å] was added as an internal standard. The recorded films were evaluated in an automatic film scanner. Unit cell parameters were refined with the program PIRUM.<sup>[14]</sup> Illustrations have been produced by using the program DIAMOND.<sup>[15]</sup>

Further details on the crystal-structure investigation may be obtained from the Fachinformationszentrum Karlsruhe, 76344 Eggenstein-Leopoldshafen, Germany (fax: (+49) 7247-808-666; e-mail: crysdata@fiz-karlsruhe.de), on quoting the depository numbers CSD-413823, CSD-413824, and CSD-413825.

Received: March 15, 2004 [Z460001]

Published Online: June 23, 2004

**Keywords:** cluster compounds · host–guest systems · supramolecular chemistry · tellurium

- [1] P. Millet, M. Johnsson, V. Pashchenko, Y. Ksari, A. Stepanov, F. Mila, *Solid State Ionics* **2001**, 141–142, 559–565.
- [2] M. Johnsson, K. W. Törnroos, P. Lemmens, P. Millet, *Chem. Mater.* **2003**, 15, 68–73.
- [3] C. Platte, M. Trömel, *Acta Crystallogr. Sect. B* **1981**, 37, 1276–1278.
- [4] C. R. Feger, G. L. Schimek, J. W. Kolis, *J. Solid State Chem.* **1999**, 143, 246–253.
- [5] G. Perez, F. Lasserre, J. Moret, M. Maurin, *J. Solid State Chem.* **1976**, 17, 143–149.
- [6] Note that the ratio of the contact distances between the cages along the [111] and [100] directions is 0.887, the ratio between a cubic axis and half its body diagonal. This difference leads to two different center-to-vertex distances for the cage atoms. Distortions such as these invariably occur when icosahedral clusters pack densely with translational symmetry.
- [7] T. F. Semenova, I. V. Rozhdestvenskaya, S. K. Filatov, L. P. Vergasova, *Mineral. Mag.* **1992**, 56, 241–245.
- [8] D. Putzas, H. W. Rotter, G. Thiele, K. Brodersen, G. Pezzeti, *Z. Anorg. Allg. Chem.* **1991**, 595, 193–202.
- [9] J. Spandl, C. Daniel, I. Brüdgam, H. Hartl, *Angew. Chem.* **2003**, 115, 1195–1198; *Angew. Chem. Int. Ed.* **2003**, 42, 1163–1166.
- [10] A. Müller, H. Reuter, S. Dillinger, *Angew. Chem.* **1995**, 107, 2505–2539; *Angew. Chem. Int. Ed. Engl.* **1995**, 34, 2328–2361.
- [11] SMART, Version 5.054 Bruker AXS Inc., Madison, Wisconsin, USA, **1999**.
- [12] SAINT, Version 6.28a Bruker AXS Inc., Madison, Wisconsin, USA, **2002**.
- [13] SHELXTL, Version 6.12 Bruker AXS Inc., Madison, Wisconsin, USA, **2001**.
- [14] P. E. Werner, PIRUM, *Ark. Kemi* **1969**, 31, 513–516.
- [15] K. Brandenburg, DIAMOND. Release 2.1e. Crystal Impact GbR, Bonn, Germany, **2000**.